ELSEVIER

J. Non-Newtonian Fluid Mech. 109 (2003) 157–176

Journal of Non-Newtonian Fluid Mechanics

www.elsevier.com/locate/jnnfm

Measurement of the temperature rise in non-Newtonian oscillatory pipe flows

J.R. Herrera-Velarde [a], R. Zenit [b], B. Mena [b,*]

[a] *Instituto Tecnológico de Zacatepec, Av. Instituto Tecnológico No. 27, Zacatepec Morelos 67980, Mexico*
[b] *Instituto de Investigaciones en Materiales, Universidad Nacional Autónoma de México, Apdo. Postal 70-360, Cd. Universitaria, Coyoacán, Mexico DF 04510, Mexico*

Received 10 January 2001; received in revised form 27 October 2002

Abstract

An experimental investigation of the temperature increase due to viscous dissipation in an oscillating pipe flow is presented. An oscillating pipe of circular section, acting as an extrusion die, was placed at the last stage of a polymer extrusion process and the increase in the temperature of the fluid, due to the superimposed oscillation, was measured. Thermocouples and a temperature control system were mounted on the walls of the oscillating section. Experimental results were obtained following the conditions suggested by Casulli et al. [J. Polym. Eng. Sci. 30 (1990) 1551]. Commercially available low density polyethylene was chosen as the experimental fluid. Results were obtained for the case when the imposed oscillatory motion was parallel to the axial direction of the flow.

The bulk temperature of the fluid at the exit of the oscillating section was found to increase with the oscillating frequency and amplitude. If the dimensionless temperature increase is plotted as a function of the characteristic oscillation speed, the experimental results collapse into a single curve.

In order to justify the experimental measurements, a theoretical analysis was performed for two simple non-Newtonian fluid models: linear viscoelastic and power-law liquids. Analytic expressions for the velocity and temperature fields were obtained. These models predicted an increase of the bulk temperature with the speed of oscillation in agreement with the experimental results. The direct comparison of the measurements and the predictions showed good order-of-magnitude agreement. We found that the temperature increase predicted using a linear viscoelastic model agrees well with the experiments for low oscillation speeds. For the case of large oscillation speeds, the prediction based on a power-law model resulted in a better agreement than the viscoelastic model prediction.

Keywords: Heat transfer; Oscillating flow; Viscoelasticity

1. Introduction

Most studies involving the flow of a viscoelastic fluid in pipes assume an isothermal state; however, in practice, many flows are far from this situation. The combination of high viscosities and large velocity

* Corresponding author.

0377-0257/02/$ – see front matter © 2002 Elsevier Science B.V. All rights reserved.
PII: S0377-0257(02)00167-2

gradients may result in a significant increase of the fluid temperature due to viscous dissipation. This effect is used, in fact, in extrusion processes where the temperature increase accelerates the melting of the material. It is believed that a complete model to describe the behavior of a viscoelastic material not only depends upon the deformation and history of deformations but also upon the temperature and the history of temperatures [2].

Heat transfer in pipes has been extensively studied for the case of Newtonian fluids. Early on, Graetz [3] solved the classic problem of forced heat convection in a pipe subjected to different boundary conditions, neglecting axial conduction.

In the particular case of oscillatory flows, the isothermal case has been studied in depth by Casulli et al., and Manero and co-workers [1,4–6]. Imposing longitudinal oscillations on a viscoelastic fluid, the velocity fields and the pressure drop changes were studied.

Studies that involve non-Newtonian flows with heat transfer effects are less numerous. Etemad and Mujumdar [7] numerically solved the heat transfer problem for a semi-circular conduit for a power-law type fluid considering a viscous dissipation and a temperature-dependent viscosity model. The results obtained showed that the Nusselt number increased for the case of constant wall temperature. This study indicates the importance of the non-Newtonian characteristics of the fluid in the heat transfer processes. Min et al. [8,9] studied numerically the developing flow of a Bingham fluid with a constant wall temperature, considering viscous dissipation and a viscosity model proposed by Papanastasiou [10]. It was found that the thermal entrance length is reduced with the yield stress of the Bingham fluid. More recently, Isayev et al. [11] and Wong et al. [12] studied theoretically and experimentally the effect of oscillations in the extruding die in a polymer melt process including some non-isothermal effects. Their results include the influence of the oscillation on the mean temperature of the extruded polymer. For the non-isothermal case they conclude that there is a temperature increase in the polymer resulting from the oscillations; the viscous dissipation resulting from the oscillations is larger than that caused by the pressure gradient across the die for the case of large amplitude oscillations; the conduction of heat dominates for the case of low mass flow rates. Other more recent studies that consider the effects of oscillation in the heat transfer phenomena include Dunwoody [13] and Ding et al. [14] who examined the inertial effects on the viscous dissipation in oscillatory shear flows.

This paper presents an experimental study in which the pipe oscillates in the main direction of the flow. In addition to the measurement of the temperature rise within the pipe, proper analytical expressions were obtained for two ‘simple’ non-Newtonian models: a linear viscoelastic fluid and a power-law fluid. The comparison of the experimental measurements and the predictions was used as an order-of-magnitude validation test. To our knowledge, measurements of the temperature increase in non-Newtonian oscillatory flows have not been reported to date.

2. Problem definition

Consider the flow in a pipe with circular cross-section of radius r resulting from a uniform pressure gradient ∇P in the axial direction of the pipe, z. Additionally, the pipe oscillates in the direction parallel to the flow imposing an additional shear stress to the fluid. The oscillation speed is $A\omega \exp(\mathrm{i}\omega t)$. The temperature of the working fluid at the entrance of the pipe and the wall temperatures are all constant, with a value T_0. A schematic diagram of the flow is shown in Fig. 1.

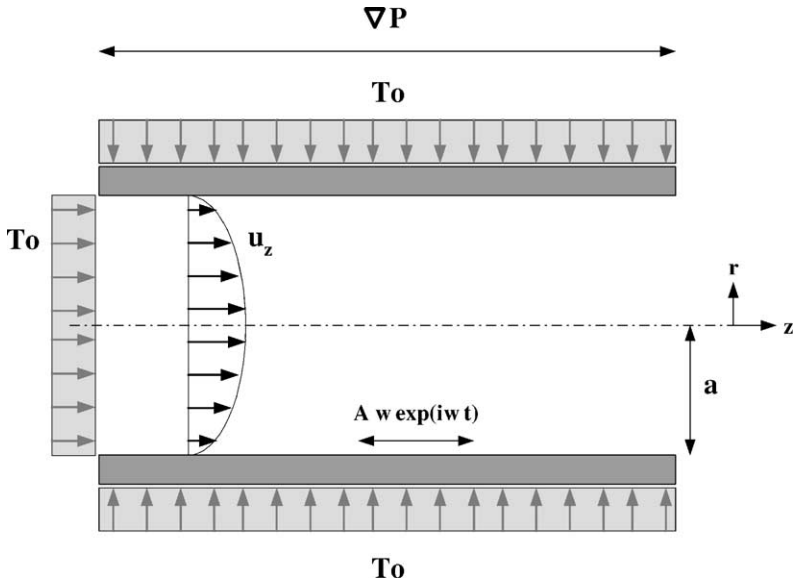

Fig. 1. Schematic of the flow entering the oscillating die with a developed velocity profile, a mean temperature T_0 and subjected to a oscillating wall with constant temperature T_0.

3. Experimental measurements of the temperature increase

An experimental set-up was designed in order to measure the temperature increase of a polymer flowing in an oscillating pipe with the same conditions as those shown in Fig. 1.

3.1. Experimental arrangement

The experimental set-up is shown in Fig. 2. A laboratory polymer extrusion machine (Haake Rheocord EU-3V extruder) was used to produce the polymer melt. An oscillating die mechanism was coupled to the exit of the extruder. This mechanism imposed an oscillatory motion to the pipe through which the fluid is flowing. Frequency and amplitude were controlled in order to subject the polymer melt to

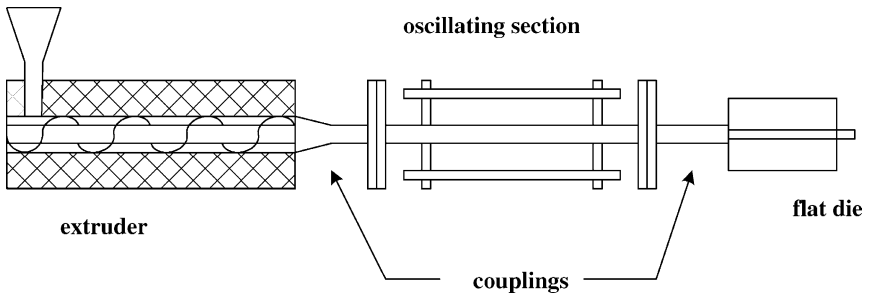

Fig. 2. Schematic of the experimental set-up.

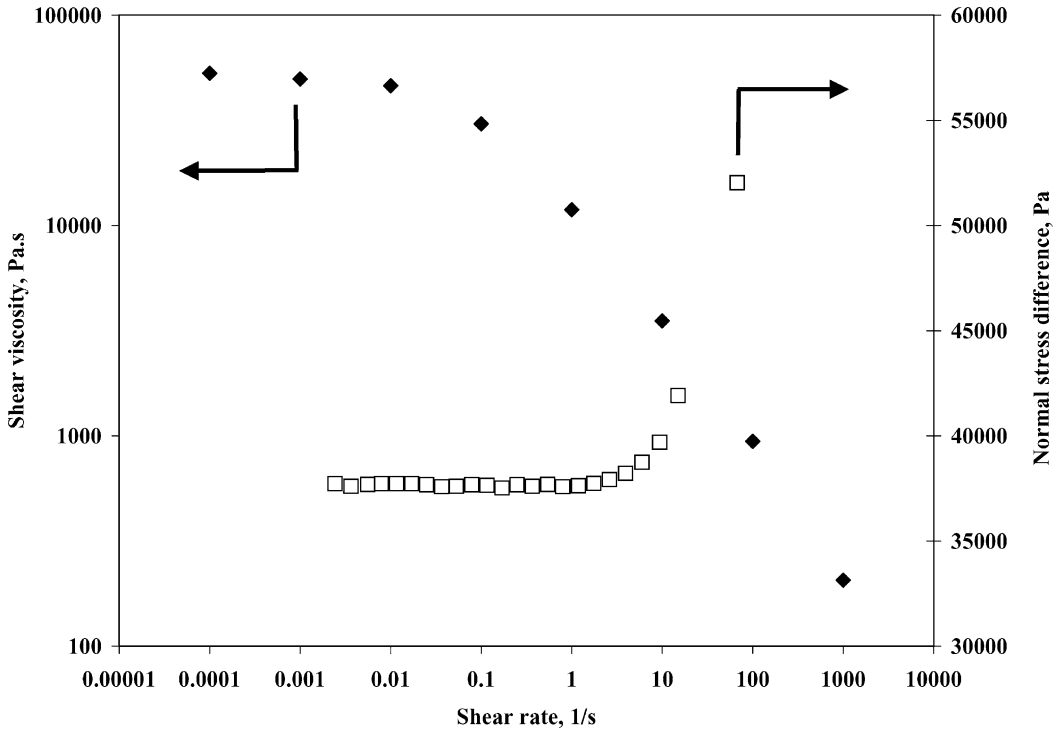

Fig. 3. Physical properties of the low density polyethylene (LDPE); taken from [15] at $T = 150\,^{\circ}\mathrm{C}$.

different flow conditions. Oscillations were possible in either the axial direction, transversal direction (angular oscillation) or a combination of both (helicoidal oscillation). A temperature control system was used to keep a constant wall temperature. Thermocouples were placed in several axial positions along the oscillating section. The temperature increase of the fluid was measured by another thermocouple at the exit of the oscillating section.

The test fluid used was low density polyethylene (LDPE), since it is a well-characterized material. The properties of the LDPE used were obtained from property tables [15]. The rheological properties of the working fluid are shown in Fig. 3.

3.1.1. Oscillating die

A schematic diagram of the oscillating section is shown in Fig. 4. The oscillating section was mounted on a series of shafts and bearings that guided the motion in the axial or angular direction. The oscillatory motion was produced by a lever-arm mechanism coupled to a dc motor. By adjusting the mechanism and the rotation speed of the motor, different oscillating conditions were available. A separate motor and mechanism set was used to produce the motion in each direction. The oscillating pipe was made of stainless steel, with an inner diameter, $2a$, of 6.8 mm and with a highly polished finish. The outer diameter was 12.7 mm and the total length was 300 mm. The coupling between the oscillating section and the non-oscillating nozzle from the extruder had a tolerance of 0.05 mm which was enough to avoid leakage and allow the motion of the oscillating section.

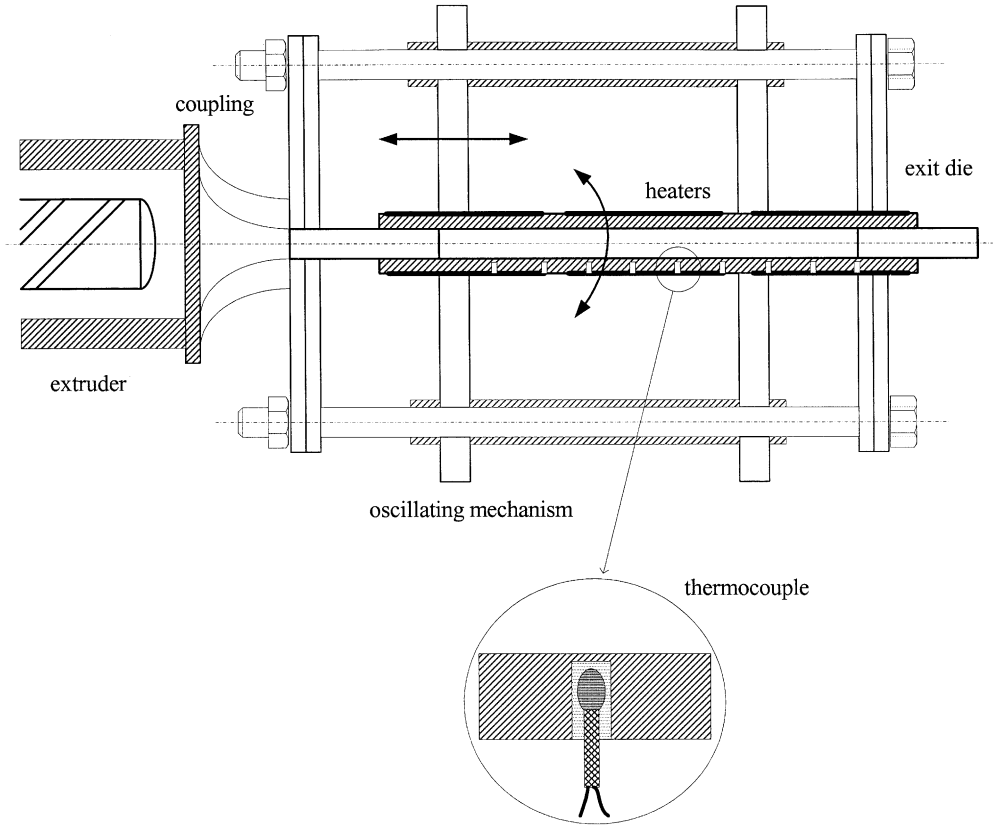

Fig. 4. Schematic of the oscillating die.

The oscillating pipe was surrounded by three flexible electric heaters (120 W each) connected to a control system (temperature controller OMROM model E5CJ). The measurement of the wall temperature was performed with type T thermocouples (copper-constant) of gauge 40 wire (0.08 mm) with a time response of 0.1 s and an accuracy of ± 0.5 K. The bare head thermocouples were embedded axially along the wall of the oscillating pipe in bore holes of 1.6 mm in diameter and 2.5 mm in depth. A total of 10 temperature gauges were used. To ensure a good thermal contact with the wall, the head of the thermocouples was immersed in silicon grease. The holes were spaced 25 mm from each other. Half of the temperature gauges were used as feedback for the control system and the rest were used to monitor the temperature directly. The temperatures were recorded using a computer-based data acquisition system. The measurement of the fluid temperature was obtained with an additional thermocouple that was centrally located at the exit of the oscillating section.

Results presented here are restricted to the case of oscillations in the axial direction, since direct comparisons are to be drawn with our theoretical predictions. The range of conditions for which the experiments were performed are presented in Table 1 and were chosen based on previous conditions used by Casulli et al. [1].

Table 1
Set of experimental conditions

Frequency (Hz)/amplitude	1 mm	2 mm	3 mm	4 mm	5 mm
1	(1, 1)	(2, 1)	(3, 1)	(4, 1)	(5, 1)
2	(2, 1)	(2, 2)	(3, 2)	(4, 2)	(5, 2)
3	(3, 1)	(2, 3)	(3, 3)	(4, 3)	(5, 3)
4	(4, 1)	(2, 4)	(3, 4)	(4, 4)	(5, 4)
5	(5, 1)	(2, 5)	(3, 5)	(4, 5)	(5, 5)
6	(6, 1)	(2, 6)	(3, 6)	(4, 6)	(5, 6)
7	(7, 1)	(2, 7)	(3, 7)	(4, 7)	(5, 7)
8	(8, 1)	(2, 8)	(3, 8)	(4, 8)	(5, 8)
9	(9, 1)	(2, 9)	(3, 9)	(4, 9)	(5, 9)
10	(10, 1)	(2, 10)	(3, 10)	(4, 10)	(5, 10)

For all the present experimental results the wall temperature was kept at $T_0 = 433\,\mathrm{K}$. The rotation speed of the extruder controlling the flow rate through the system was also kept constant at a value of 30 rpm. The volumetric flow rate for this conditions was $Q = 1.5 \times 10^{-8}\,\mathrm{m^3/s}$.

A given set of experiments starts with the lowest frequency for a given amplitude. Once the experiment achieves a steady state, approximately 20 min, the measurements are recorded and the frequency is increased to the next desired value, keeping the amplitude constant.

The experimental results are presented in terms of the dimensionless temperature defined as

$$\theta = \frac{T_\mathrm{c} - T_0}{T_0},$$

where T_c is the measured temperature in the center of the channel and T_0 is the temperature of the wall.

3.2. Experimental results

Fig. 5 shows the dimensionless temperature as a function of the oscillation frequency for experiments at different amplitudes. The error involved in the measurement is depicted by the vertical line shown on one data point at the left of the figure. Although the error involved in the measurements is significant, as in most heat transfer experiments, the experimental trend can be clearly observed. For small amplitudes and low frequencies, the temperatures obtained were below the minimum measurable scale; hence, they are not reported.

Clearly, the temperature of the fluid increases with the frequency of oscillation. For a given oscillation frequency, the temperature increase is larger for larger oscillation amplitudes. The measured values of the dimensionless temperatures are of the order of 10^{-3} which corresponded to a temperature increase of the order of 10°.

Fig. 6 shows the experimental results in terms of the dimensionless oscillation speed, α^*, defined as

$$\alpha^* = \frac{\omega A}{\bar{u}_z},$$

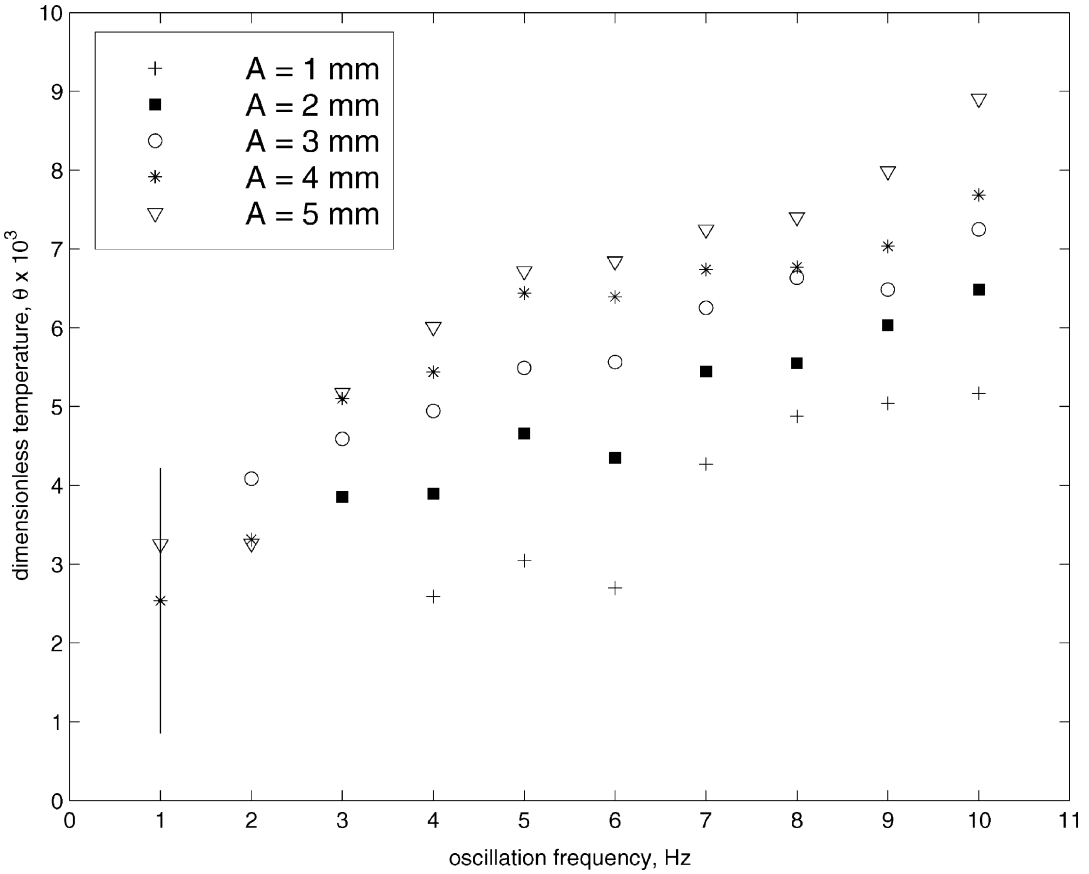

Fig. 5. Dimensionless temperature θ as function of the oscillation frequency ω for different values of the oscillation amplitude A for LDPE. The size of the error bar in the first data point on the left denotes the typical error associated with the measurement: $T_0 = 433\,\mathrm{K}$ and $Q = 1.5 \times 10^{-8}\,\mathrm{m^3/s}$.

where A is the oscillation amplitude, ω the oscillation frequency and $\bar{u}_z$ is the mean velocity inside the pipe

$$\bar{u}_z = \frac{Q}{A'},$$

where A' is the cross-section area of the pipe. Note that the dimensionless oscillation speed is of order 1, the same order as the mean pressure-driven fluid velocity. The theoretical predictions have been obtained for this particular range of dimensionless oscillation speeds.

The experimental results presented in this manner appear to collapse onto a single curve. Clearly, the relevant parameter that controls the fluid temperature increase is the dimensionless oscillation speed. The temperature increases rapidly for small values of the dimensionless oscillation speed but does not increase significantly for values of α^* larger than 6.

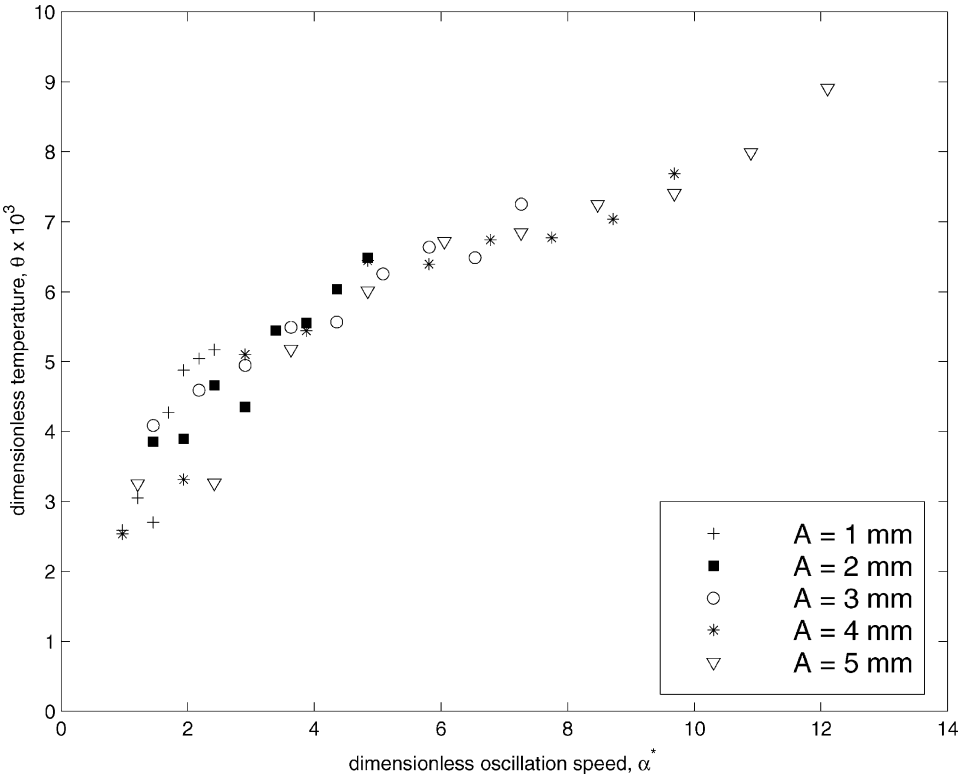

Fig. 6. Dimensionless temperature θ as function of the dimensionless oscillation speed α^* for LDPE: $T_0 = 433\,\mathrm{K}$ and $Q = 1.5 \times 10^{-8}\,\mathrm{m^3/s}$.

4. Theoretical predictions

Consider the conservation equations for an incompressible liquid,

$$\nabla \cdot \vec{u} = 0, \tag{1}$$

$$\rho\left(\frac{\partial \vec{u}}{\partial t}\right) = -\nabla P + \nabla \cdot \tilde{\tau}, \tag{2}$$

$$\rho C_p(\vec{u} \cdot \nabla T) + \nabla \cdot (k\nabla T) = \tilde{\tau} : \nabla \vec{u}, \tag{3}$$

where $\vec{u}$ is the velocity vector, P the scalar pressure, $\tilde{\tau}$ the extra stress tensor, ρ the mass density, C_p the specific heat, k the thermal conductivity and T is the temperature.

For the geometry shown in Fig. 1, the velocity vectors are $u_r = 0, u_\theta = 0$ and $u_z = u(r, z)$, which satisfy the equation of continuity (Eq. (1)) exactly. The conservation of momentum (Eq. (2)) in the z-direction is reduced to

$$\rho\frac{\partial u_z}{\partial t} = G + \frac{1}{r}\frac{\partial}{\partial r}(r\tau_{rz}), \tag{4}$$

where $G = -\partial P/\partial z$ is the constant pressure gradient and τ_{rz} is the component of the stress tensor in the axial direction of the pipe. The boundary conditions for this equation are

1. $u_z = \alpha\Re\{\exp(\mathrm{i}\omega t)\}$ at $r = a$;
2. $\partial u_z/\partial r = 0$ at $r = 0$.

α is the oscillation speed and can be expressed is terms of the oscillation frequency ω and the oscillation amplitude A, as

$$\alpha = \omega A. \tag{5}$$

Eq. (3), for a fully developed temperature field for the same flow, neglecting the axial conduction, reduces to

$$\rho C_p u_z \left(\frac{\partial T}{\partial z}\right) = k\frac{1}{r}\frac{\partial}{\partial r}\left(r\frac{\partial T}{\partial r}\right) + \tau_{rz}\left(\frac{\partial u_z}{\partial r}\right). \tag{6}$$

We consider that the temperature profile of the fluid is constant with T_0 at the entrance of the oscillating wall. The oscillating wall temperature is also held constant at T_0. Hence, the boundary conditions are given by

1. $T = T_0$ at $r = a$ for all z;
2. $\partial T/\partial r = 0$ at $r = 0$ for all z.

The above set of equations can be solved if a model for the rheological behavior is given. In the following section a linear viscoelastic and a generalized Newtonian models are considered.

4.1. Linear viscoelastic model

The viscoelastic state can be characterized by the form of the stress tensor

$$\tau_{ij} = -Pg_{ij} + \tilde{\tau}_{ij}, \tag{7}$$

where the extra stress tensor $\tilde{\tau}_{ij}$ is given as a function of the relaxation or memory function Ψ as:

$$\tilde{\tau}_{ij} = 2\int_{-\infty}^{t} \Psi(t - t')e_{ij}(x, t')\,\mathrm{d}t', \tag{8}$$

where

$$\Psi(t - t') = \int \frac{N(\zeta)}{\zeta}\exp\left(-\frac{t - t'}{\zeta}\right)\mathrm{d}\zeta. \tag{9}$$

Following the usual notation, τ_{ij} is the stress tensor, P the isotropic pressure, g_{ij} the metric tensor of a fixed coordinate system, e_{ij} the rate of strain tensor and $N(\zeta)$ is the relaxation spectrum.

The liquid represented in Eqs. (7) and (9) falls into the framework of the general equations of linear viscoelasticity [16]. It contains, as a special case, the Jeffreys model by setting

$$N(\zeta) = \eta_0\frac{\lambda_1}{\lambda_2}\delta(\zeta) + \eta_0\frac{\lambda_1 - \lambda_2}{\lambda_1}\delta(\zeta - \lambda_1), \tag{10}$$

where η_0 is the zero shear rate viscosity, λ_1 and λ_2 the relaxation and retardation time, respectively, and δ represents a Dirac delta function. Clearly, if $\lambda_2 = 0$, a Maxwell type constitutive equation is recovered,

and if $\lambda_1 = \lambda_2$ the purely viscous case is represented. This model is sometimes known as the Oldroyd model.

The equation of motion (Eq. (4)) can be made homogeneous using as dependent variable the departure velocity from the steady state value

$$w(r,t) = u(r,t) - \left(\frac{G}{4\eta_0}\right)(a^2 - r^2), \tag{11}$$

where G is the pressure gradient in the axial direction. Hence,

$$\frac{\partial u_z}{\partial t} = \frac{\eta_0}{\rho}\left(\frac{\partial^2 u_z}{\partial r^2} + \frac{1}{r}\frac{\partial u_z}{\partial r}\right). \tag{12}$$

With boundary conditions $u_z(a,t) = \alpha\exp(\mathrm{i}\omega t)$ and $(\partial/\partial r)u_z(0,t) = 0$. This problem can be solved by a separation of variables scheme. Herrera-Velarde and Mena [17] obtained the velocity field

$$u_z = \alpha\frac{J_0[Kr]}{J_0[Ka]}\exp(\mathrm{i}\omega t) + \frac{G}{4\eta_0}(a^2 - r^2), \tag{13}$$

where J_0 is the Bessel function of order zero and K is a constant defined as

$$K = \left(\frac{\omega\rho}{\eta_0}\right)^{1/2}\left(\frac{-\mathrm{i}(1+\mathrm{i}\omega\lambda_1)}{1+\mathrm{i}\omega\lambda_2}\right)^{1/2}, \tag{14}$$

where λ_1 and λ_2 are the relaxation and retardation time, respectively.

To observe the effect of the oscillations in the flow, the Reynolds number of the non-oscillating flow is made to be the same as that of the oscillating part of the flow,

$$\frac{2\rho\langle u_\mathrm{p}\rangle a}{\eta_0} \approx \frac{2\rho\alpha a}{\eta_0},$$

where $\langle u_\mathrm{p}\rangle$ is the average velocity of the non-oscillating pipe flow (Poiseuille flow). Hence, for this case the oscillation speed $\alpha = \omega A$ has to be of the same order as $\langle u_\mathrm{p}\rangle$.

A dimensionless velocity is defined as

$$\frac{u_z}{u_m} = \frac{\alpha}{u_m}\frac{J_0[Kr]}{J_0[Ka]}\exp(\mathrm{i}\omega t) + \left(1 - \frac{r^2}{a^2}\right), \tag{15}$$

where $u_m = Ga^2/(4\eta_0)$ is the maximum velocity of the non-oscillatory Poiseuille flow. Plots of the velocity field for different values of the $\omega\lambda_1$ and $\omega\lambda_2$ can be found in [17,19].

Now, we can solve for the laminar forced heat convection of the flow. Assuming a fully developed temperature profile with a constant temperature gradient in the axial direction and using Eqs. (3) and (8), the energy balance can be written as

$$\rho C_p u_z \cdot \frac{\Delta T}{\Delta Z} = k\frac{1}{r}\frac{\mathrm{d}}{\mathrm{d}r}\left(r\frac{\mathrm{d}T}{\mathrm{d}r}\right) + \eta_0\left(\frac{1+\mathrm{i}\omega\lambda_1}{1+\mathrm{i}\omega\lambda_2}\right)\left(\frac{\mathrm{d}u_z}{\mathrm{d}r}\right)^2. \tag{16}$$

Using the velocity profile $u_z = u_z(r,t)$ (Eq. (13)) and the boundary conditions for the temperature field,

the above equation can be integrated to yield

$$T = T_0 + C_3\left\{\int \frac{1}{r}\left(\int r' u_z(r')\mathrm{d}r'\right)\mathrm{d}r - \left[\int \frac{1}{r}\left(\int r' u_z(r')\mathrm{d}r'\right)\mathrm{d}r\right]_{r=a}\right\}$$
$$- C_4\left\{\int \frac{1}{r}\left(\int r'\left(\frac{\partial u_z(r')}{\partial r'}\right)^2 \mathrm{d}r'\right)\mathrm{d}r - \left[\int \frac{1}{r}\left(\int r'\left(\frac{\partial u_z(r')}{\partial r'}\right)^2 \mathrm{d}r'\right)\mathrm{d}r\right]_{r=a}\right\}, \quad (17)$$

where

$$C_3 = \frac{\rho C_p}{k}\left(\frac{\Delta T}{\Delta z}\right),$$

and

$$C_4 = \frac{\eta_0}{k}\left(\frac{1+\mathrm{i}\omega\lambda_1}{1+\mathrm{i}\omega\lambda_2}\right).$$

The above equation may be solved analytically resulting in

$$T - T_0 = C_3\left(-\frac{C_1}{K^2}(J_0(Kr) - J_0(Ka)) + \frac{C_2}{16}(4a^4r^2 - r^4 - 3a^4)\right)$$
$$- \frac{C_4}{4K^2}(2C_1^2K^4((rJ_1(Kr))^2 - (aJ_1(Ka))^2) - 2C_1^2K^3(rJ_0(Kr)J_1(Kr) - aJ_0(Ka)J_1(Ka))$$
$$+ 2C_1^2K^4((rJ_0(Kr))^2 - (aJ_0(Ka))^2) + 2C_1^2K^2((J_0(Kr))^2 - (J_0(Ka))^2) - 32C_1C_2(J_0(Kr)$$
$$- J_0(Ka)) - 16C_1C_2\,K(rJ_1(Kr) - aJ_1(Ka)) + C_2^2K^2(r^4 - a^4), \quad (18)$$

where J_0 and J_1 are the Bessel functions of order 0 and 1, respectively. Also,

$$C_1 = \alpha\frac{\exp(\mathrm{i}\omega t)}{J_0(Ka)},$$

and

$$C_2 = \frac{G}{4\eta_0},$$

which arise from writing the velocity profile as

$$u_z = C_1J_0(Kr) + C_2(a^2 - r^2).$$

Fig. 7 shows the cycle-averaged dimensionless temperature profiles for three different values of the axial temperature gradient. The dimensionless temperature is defined as

$$\theta = \frac{T - T_0}{T_0}.$$

The effect of the elasticity of the fluid can be observed. When the difference between the relaxation and retardation times ($\omega\lambda_1$ and $\omega\lambda_2$) is large, the deviation from the Newtonian temperature profile is

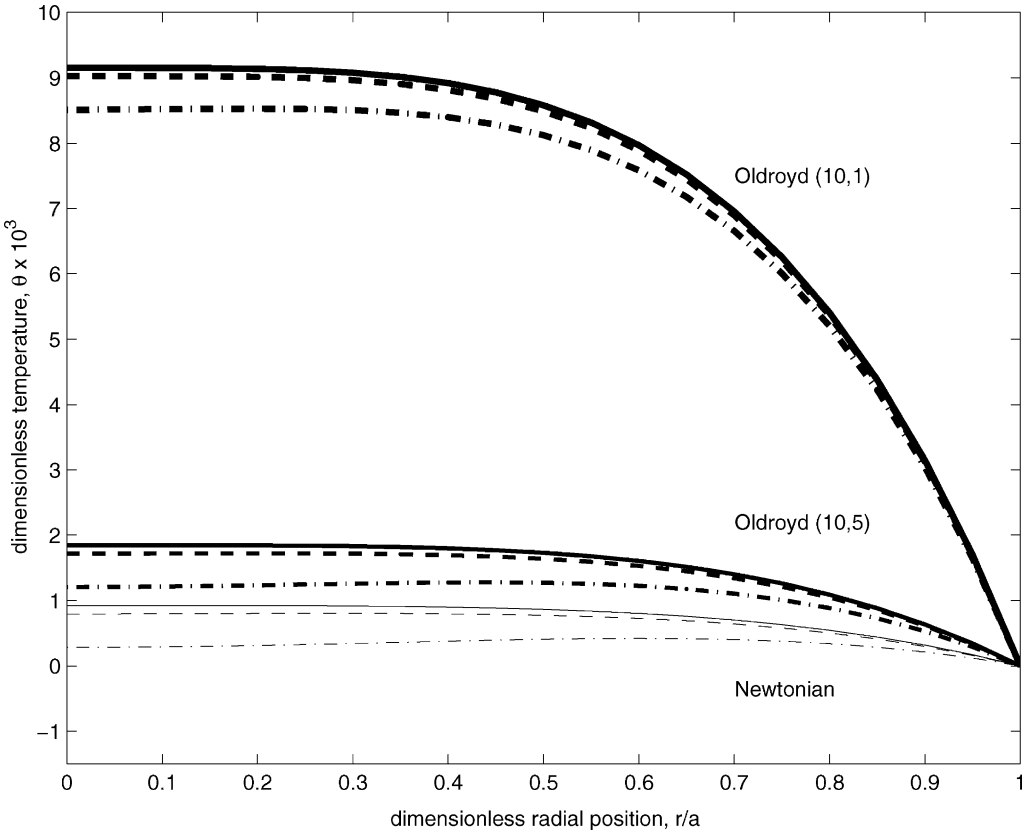

Fig. 7. Dimensionless temperature θ as a function of dimensionless radial position for a Oldroyd fluids. Three different fluids are shown: (1) thin lines, Newtonian fluid; (2) medium thickness lines, Oldroyd fluid, $\omega\lambda_1 = 10$, $\omega\lambda_2 = 5$; (3) thick lines, Oldroyd fluid, $\omega\lambda_1 = 10$, $\omega\lambda_2 = 1$. The solid, dashed and dashed-dotted lines show the predictions for values of $\Delta T/\Delta z = 0$, 1 and 5 K/m, respectively. For this case $u_m = \alpha = 1 \times 10^{-2}$ m/s ($a = 1 \times 10^{-3}$ m, $\eta_0 = 1 \times 10^3$ Pa s, $\omega = 10$/s and $A = 1 \times 10^{-3}$ m), $C_p = 1 \times 10^3$ kJ/(kg K), $T_0 = 4 \times 10^2$ K, $\rho = 1 \times 10^3$ kg/m^3, $k = 1 \times 10^{-1}$ W/m^2 K.

larger. Also, for all cases, as the axial temperature gradient increases, the dimensionless temperature decreases.

To analyze the effect of the oscillation speed, the condition of ($\alpha = \langle u_p \rangle$) is relaxed, therefore, the bulk temperature can be calculated for different oscillation speed values. The dimensionless bulk temperature is defined as

$$\theta_b = \frac{\bar{T} - T_0}{T_0} \tag{19}$$

where $\bar{T}$ is the cycle-averaged temperature

$$\bar{T} = \frac{\int_0^{2\pi} \int_0^a u_z(r,t) T(r,t)\, \mathrm{d}r\, \mathrm{d}(\omega t)}{\int_0^{2\pi} \int_0^a u_z(r,t)\, \mathrm{d}r\, \mathrm{d}(\omega t)}. \tag{20}$$

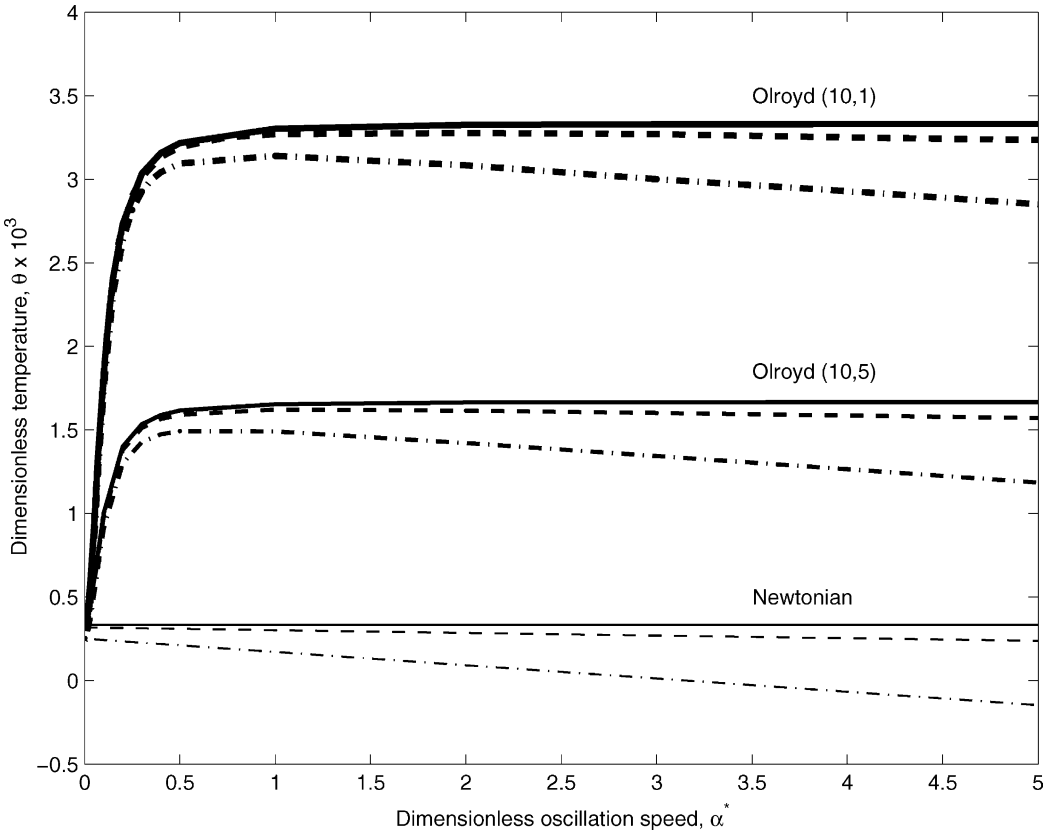

Fig. 8. Dimensionless bulk temperature θ_b, as a function of the normalized oscillation velocity $\omega A/u_m$. Three different fluids are shown: (1) thin lines, Newtonian fluid; (2) medium thickness lines, Oldroyd fluid, $\omega\lambda_1 = 10$, $\omega\lambda_2 = 5$; (3) thick lines, Oldroyd fluid, $\omega\lambda_1 = 10$, $\omega\lambda_2 = 1$. The solid, dashed and dashed-dotted lines show the predictions for values of $\Delta T/\Delta z = 0$, 1 and 5K/m, respectively. The material parameters are the same as those used in Fig. 7.

Fig. 8 shows the dimensionless bulk temperature as a function of the dimensionless oscillation speed α^* defined as

$$\alpha^* = \frac{\omega A}{u_m}. \tag{21}$$

The dimensionless temperature appears to reach an asymptotic value as the dimensionless oscillation velocity increases. The temperature appears to be independent of the oscillation velocity for the case of a Newtonian fluid; on the other hand, as the fluid becomes more viscoelastic, the magnitude of the oscillation causes an increase of the dimensionless temperature. The temperature is, again, inversely proportional to the value of the axial temperature gradient.

4.2. Generalized Newtonian model

The generalized Newtonian model considers a modified viscosity–shear rate relationship to account for the case in which the viscosity of the fluid depends on the shear rate. A well-known generalized model is

the power-law model [16], in which the viscosity of the fluid depends on the magnitude of the strain rate,

$$\eta = m\dot{e}^{n-1}, \tag{22}$$

where n and m are constants characteristics of a particular fluid. The magnitude of the strain rate is defined as $\dot{e} = \sqrt{(1/2)\sum_i \sum_j e_{ij}e_{ij}}$. Hence, the ij component of the extra stress tensor is

$$\tilde{\tau}_{ij} = me_{ij}^n. \tag{23}$$

The relevant component of the stress tensor for the problem of interest is τ_{rz}, which can be expressed simply by

$$\tau_{rz} = m\left(\frac{\partial u_z}{\partial r}\right)^n. \tag{24}$$

Note that if $n = 1$, the Newtonian case is recovered where the value of m corresponds to the shear viscosity η_0.

To solve the momentum conservation (Eq. (4)) we assume that the axial velocity component u_z can be decomposed in $u_o = u_o(t)$, the motion due to the periodic oscillation of the walls, and u_p resulting from the pressure gradient,

$$u_z = u_o + u_p. \tag{25}$$

To assume that the oscillating velocity component does not depend on the coordinate r is a crude approximation; however, it allows us to obtain analytic expressions for the velocity and temperature fields. If we take $u_o = \Re\{\omega A \exp(i\omega t)\}$, Eq. (4) can be expressed as

$$i\omega^2 \rho A \exp(i\omega t) = G - \frac{1}{r}\frac{\partial}{\partial r}(r\tau_{rz}). \tag{26}$$

If the pressure gradient G is constant, the expression above can be integrated with respect to r to obtain the general solution for the component τ_{rz} of the stress tensor. With the condition that the stress must be finite at $r = 0$, we obtain

$$\tau_{rz} = (\tfrac{1}{2}r)(G + \rho i\omega^2 A \exp(i\omega t)). \tag{27}$$

Using this expression in Eq. (24), we obtain

$$\left(\frac{du_z}{dr}\right) = \left(\frac{r}{2m}\right)^{1/n} (G + i\omega^2 \rho A \exp(i\omega t))^{1/n}, \tag{28}$$

which can be integrated with respect to r to obtain the velocity profile using the wall velocity as a boundary condition, $u_z(r = a) = \alpha \exp(i\omega t)$. Hence,

$$u_z = \left(\frac{n}{1+n}\right)\left(\frac{G + i\omega\alpha\rho \exp(i\omega t)}{2m}\right)^{1/n} \left(a^{(1/n)+1} - r^{(1/n)+1}\right) + \alpha \exp(i\omega t). \tag{29}$$

For this case, a non-dimensional velocity is defined as

$$\frac{u_z}{u_m} = \left(\frac{G + i\omega\alpha \exp(i\omega t)^{1/n}}{G}\right)^{1/n} \left(1 - \left(\frac{r}{a}\right)^{(1/n)+1}\right) + \frac{\alpha \exp(i\omega t)}{(n/(1+n))(G/2m)^{1/n} a^{(1/n)+1}}, \tag{30}$$

where u_m is the maximum velocity for the non-oscillating Poiseuille pipe flow given by

$$u_m = \left(\frac{n}{1+n}\right)\left(\frac{G}{2m}\right)^{1/n} a^{(1/n)+1}.$$

To make the magnitude of the oscillation velocity be of the same order as that of the Poiseuille flow, the pressure gradient G is calculated in terms of the oscillation speed, α

$$\alpha \approx u_m,$$

hence

$$|G| = 2m\left(\frac{\alpha(1+n)}{na^{(1/n)+1}}\right)^n.$$

Plots of the velocity field for this expression can be found in [18,19].

The energy conservation (Eq. (6)) can be written for the generalized Newtonian fluid as

$$\rho C_p u_z \cdot \frac{\Delta T}{\Delta Z} = k\frac{1}{r}\frac{\mathrm{d}}{\mathrm{d}r}\left(r\frac{\mathrm{d}T}{\mathrm{d}r}\right) + m\left(\frac{\mathrm{d}u_z}{\mathrm{d}r}\right)^{n+1}, \tag{31}$$

which can be integrated for the given set of boundary conditions since the velocity profile (Eq. (29)) is known,

$$\begin{aligned} T = T_0 &+ C_7\left\{\int\frac{1}{r}\left(\int r' u_z(r')\mathrm{d}r'\right)\mathrm{d}r - \left[\int\frac{1}{r}\left(\int r' u_z(r')\mathrm{d}r'\right)\mathrm{d}r\right]_{r=a}\right\} \\ &- C_8\left\{\int\frac{1}{r}\left(\int r'\left(\frac{\partial u_z(r')}{\partial r'}\right)^{n+1}\mathrm{d}r'\right)\mathrm{d}r - \left[\int\frac{1}{r}\left(\int r'\left(\frac{\partial u_z(r')}{\partial r'}\right)^{n+1}\mathrm{d}r'\right)\mathrm{d}r\right]_{r=a}\right\}, \end{aligned} \tag{32}$$

where

$$C_7 = \frac{\rho C_p}{K}\left(\frac{\Delta T}{\Delta z}\right),$$

and

$$C_8 = \frac{m}{k}.$$

An analytic solution can be found for the above expression resulting in

$$\begin{aligned} T - T_0 = C_7 &\left(\frac{C_5 a^{(1/n)+1} + C_6}{4}(r^2 - a^2) - \frac{C_5 n^2}{(3n+1)^2}(r^{(1/n)+3} - a^{(1/n)+3})\right) \\ &- \frac{C_8 n^2}{(1+3n)^2}\left(\frac{C_5(n+1)}{n}\right)^{n+1}(r^{(1/n)+3} - a^{(1/n)+3}), \end{aligned} \tag{33}$$

where

$$C_5 = \left(\frac{n}{1+n}\right)\left(\frac{G + \mathrm{i}\omega\alpha\rho\exp(\mathrm{i}\omega t)}{2m}\right)^{1/n},$$

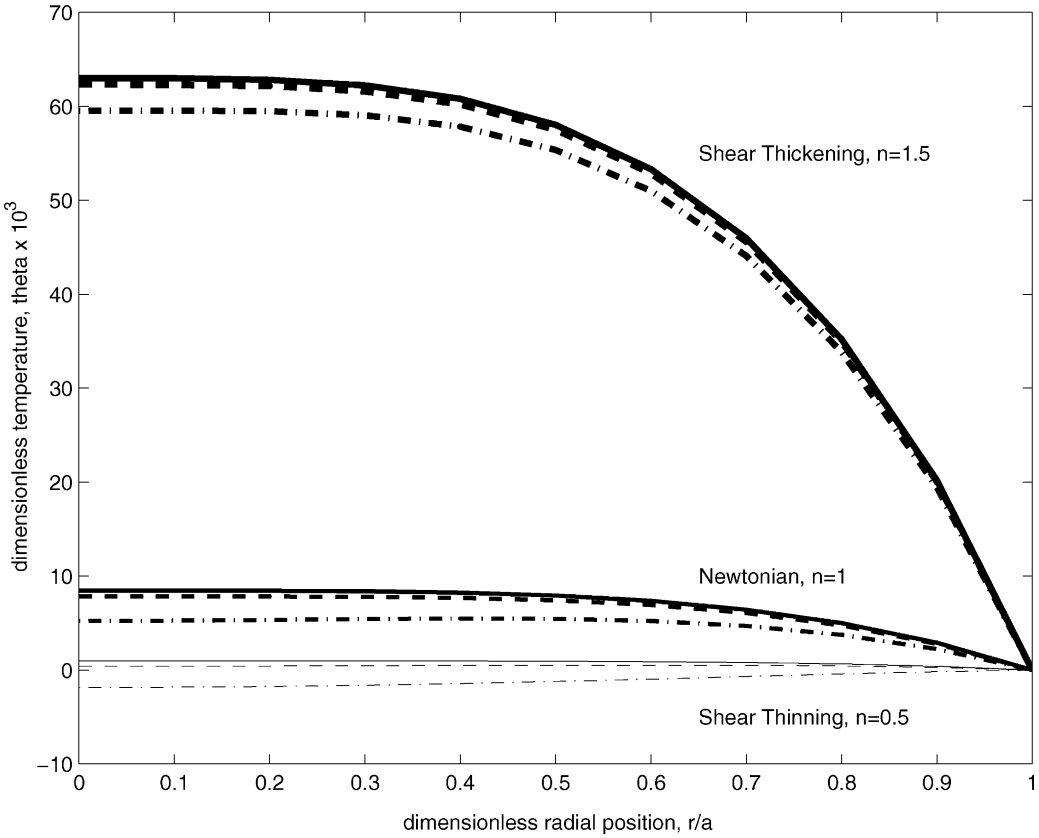

Fig. 9. Dimensionless temperature θ, as a function of dimensionless radial position for power-law fluids. Three different fluids are shown: (1) thin lines, shear thinning liquid, $n = 1/2$; (2) medium thickness lines, Newtonian fluid, $n = 1$; (3) thick lines, shear thickening liquid, $n = 1.5$. The solid, dashed and dashed-dotted lines show the predictions for values of $\Delta T/\Delta z = 0$, 1 and 5 K/m, respectively. For this case $u_m = \alpha = 1 \times 10^{-2}$ m/s ($a = 1 \times 10^{-3}$ m, $m = 1 \times 10^3$ Pa s, $\omega = 10$/s and $A = 1 \times 10^{-3}$ m), $C_p = 1 \times 10^3$ kJ/(kg K), $T_0 = 1 \times 10^2$ K, $\rho = 1 \times 10^3$ kg/m^3, $k = 1 \times 10^{-1}$ W/(m^2 K).

and

$$C_6 = \alpha \exp(\mathrm{i}\omega t).$$

The temperature profile is plotted in dimensionless form in Fig. 9 for three values of the power parameter.

Relaxing the condition that the oscillation speed be equal to the mean pipe-flow velocity, we obtain estimates of the effect of oscillation on the overall increase of temperature in the fluid. Fig. 10 shows the bulk temperature, defined in Eq. (20), for the three cases of the power coefficient and for three different values of the axial temperature gradient. For this model, the temperature increases monotonically for all cases. The shear thickening fluid attains larger temperatures than those for the Newtonian or shear thinning fluids, for the same oscillating conditions. The temperature increase shows a weak dependence on the value of the axial temperature gradient, with a small increase of θ as $\Delta T/\Delta z$ decreases.

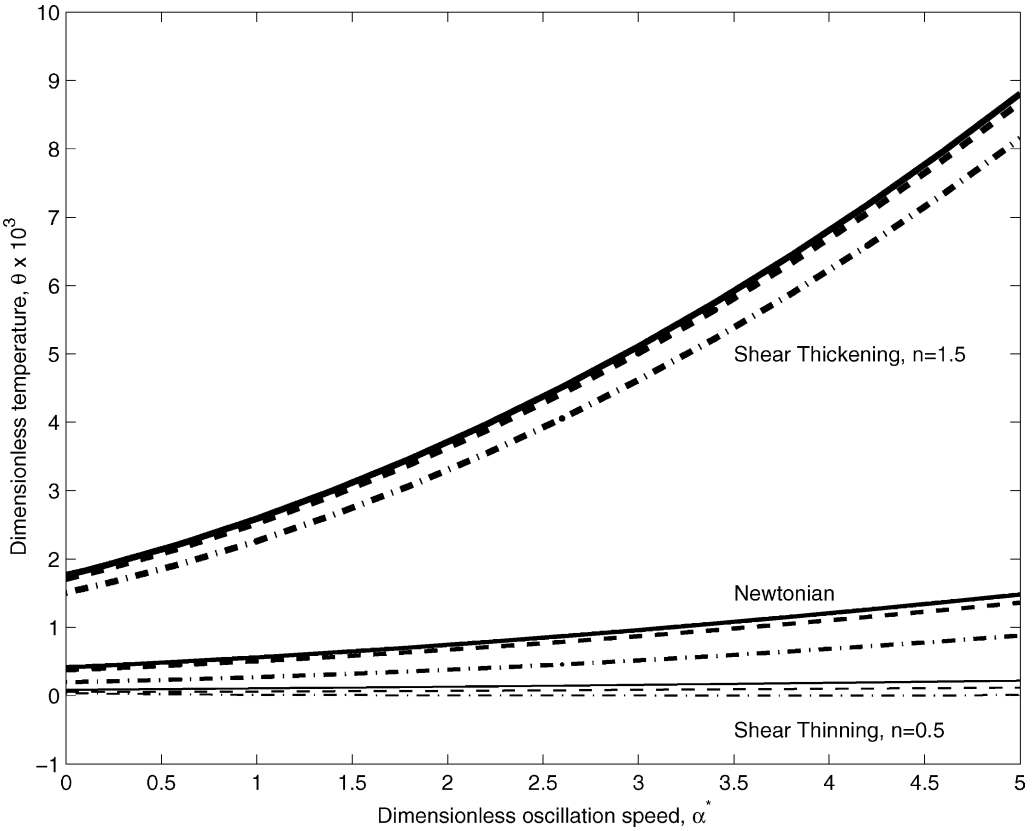

Fig. 10. Dimensionless bulk temperature θ_b, as a function of the normalized oscillation velocity $\omega A/u_m$. Three different fluid are shown: (1) thin lines, shear thinning liquid, $n = 1/2$; (2) medium thickness lines, Newtonian fluid, $n = 1$; (3) thick lines, shear thickening liquid, $n = 1.5$. The solid, dashed and dashed-dotted lines show the predictions for values of $\Delta T/\Delta z = 0$, 1 and 5 K/m, respectively. For this case the flow parameters are the same as those used in Fig. 9.

5. Comparison with theoretical predictions

A theoretical analysis of the heat transfer for two non-Newtonian liquids in an oscillating pipe was presented in Sections 4.1 and 4.2. Using the values of the properties of LDPE and the experimental parameters, a direct comparison between the theoretical expressions and the experimental measurements is possible. Results are presented in terms of the dimensionless bulk temperature (Eq. (19)) and the dimensionless oscillation speed (Eq. (21)).

The dashed line in Fig. 11 shows the prediction of Eq. (18) for a range of values of α^* using the physical properties of the LDPE. The value of the axial temperature gradient used in the predictions was found experimentally,

$$\frac{\Delta T}{\Delta z} \approx 1\,\mathrm{K/m}.$$

Predicted and experimental results agree well for dimensionless oscillation speeds below 5. It must be

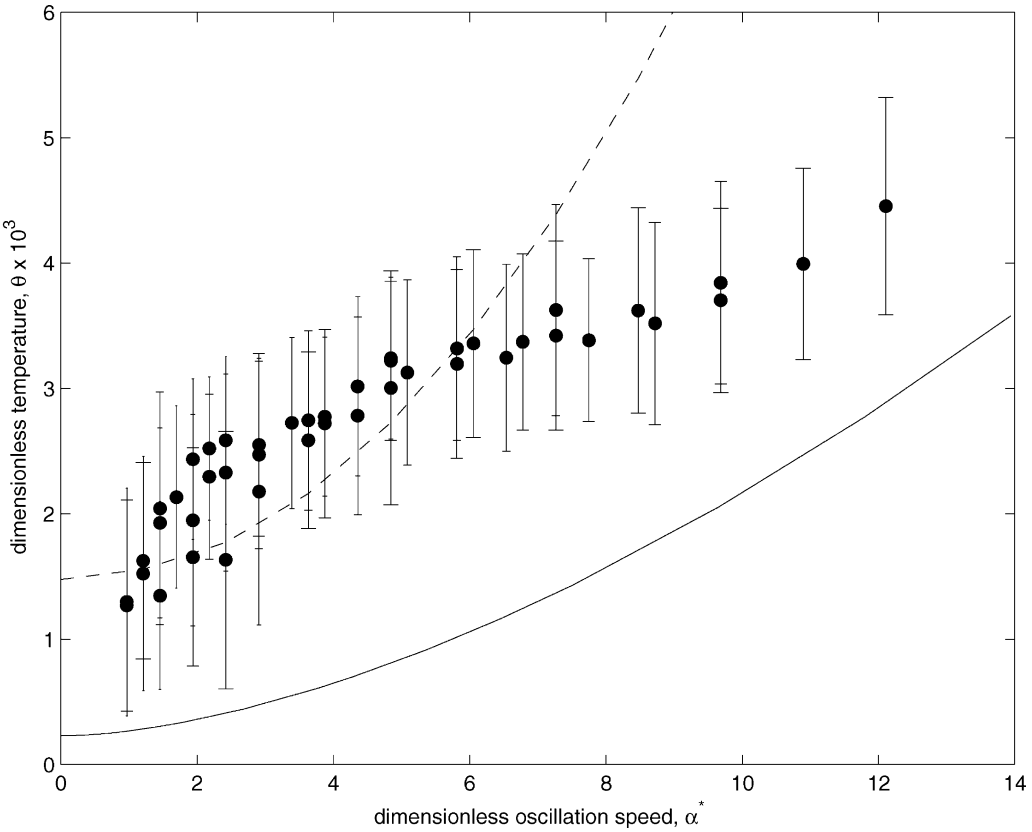

Fig. 11. Dimensionless bulk temperature θ_b as function of the dimensionless oscillation speed α^* for LDPE. Comparison between experimental measurements and the predictions based on a viscoelastic model (dashed line) and a power-law model (solid line). Property values used for the theoretical predictions: $\rho = 920.0\,\text{kg/m}^3$, $C_p = 2000.0\,\text{kJ/(kg K)}$, $k = 0.5\,\text{W/(m K)}$, $\eta_0 = 600\,\text{Pa s}$, $\lambda_1 = 5.5\,\text{s}$, $\lambda_2 = 0.01\,\text{s}$, $n = 0.47$, $m = 8202.9\,\text{N s/m}^{0.47}$.

noted that although the magnitude of the experiments and the predictions agree well, the trends observed are significantly different.

The solid line in Fig. 11 shows the theoretically predicted values of Eq. (33), considering a constant value of $\Delta T/\Delta z = 1\,\text{K/m}$. Using this theoretical model, the value of the dimensionless temperature lies below the experiments for the whole range of oscillations. For oscillation speeds larger than 12, the model and the measurements appear to agree better than for small speeds. For this model, the trend is similar to the one found in the experiments.

6. Summary and conclusions

Measurements of the temperature increase caused by viscous dissipation in an oscillatory pipe flow were obtained. Great care was taken in the experimental design to measure temperature increases of a few degrees for mean working temperatures of the order of 400 K. The increase of the fluid temperature

was found to scale with the dimensionless oscillation speed. Although this increase is not very large, it is nevertheless important for processes involving the extrusion of molten polymers. Even a small temperature variation has been known to modify significantly the surface properties of extruded products [20]. These measurements are, to our knowledge, the first of their kind.

Direct comparisons were made between theoretical predictions and experimental measurements. The prediction form these simple models give us a proper validity tests for the experimental measurements. For small values of the oscillation speed, good agreement was found between the experiments and the theoretical predictions from a linear viscoelastic model. The agreement ceased to be valid when the magnitude of the imposed oscillation was larger than the pressure gradient driving the flow. For larger values of the oscillatory speed, good agreement was found with theoretical predictions from a power-law inelastic fluid. As expected, for the intermediate range of oscillation speeds, the rheological behavior of the test fluid (LDPE) requires a constitutive equation that combines viscoelastic and shear thinning properties. It is clear that the rheological models considered in this paper are 'simple'; hence, it is expected that the behavior of LDPE cannot be fully predicted by either model. However, the simplicity of the theoretical analysis allowed us to obtain analytical expressions that could be compared in a direct manner the experimental results. Direct comparisons between experimental and theoretical results in heat transfer problems involving non-Newtonian flows are rare.

Acknowledgements

The support of PAPIIT-DGAPA of UNAM through its grants IN503494 and IN103900, and CONACYT through its scholarship program and the grant NC-204 are greatly acknowledged. J.R.H.-V. wishes to acknowledge the Instituto Tecnológico de Zacatepec for its support during the completion of his graduate studies.

References

[1] J. Casulli, J.R. Clermont, A. Von Ziegler, B. Mena, The oscillating die: a useful concept in polymer extrusion, J. Polym. Eng. Sci. 30 (1990) 1551–1556.
[2] G.W.M. Peters, F.P.T. Baaijens, Modelling of non-isothermal viscoelastic flows, J. Non-Newt. Fluid Mech. 68 (1997) 205–224.
[3] L. Graetz, Über die wärmeleitungsfähigkeit von flüssigkeiten, Ann. Phys. Chem. 18 (1883) 79–94.
[4] O. Manero, B. Mena, An interesting effect in non-Newtonian flow in oscillating pipes, Rheol. Acta 17 (1977) 573–573.
[5] O. Manero, R. Valenzuela, B. Mena, Further developments on non-Newtonian flow in oscillating pipes, Rheol. Acta 17 (1978) 693.
[6] B. Mena, O. Manero, D.M. Binding, Complex flow of viscoelastic fluids through oscillating pipes; interesting effects and applications, J. Non-Newt. Fluid Mech. 5 (1979) 427–447.
[7] S.G. Etemad, H. Mujumdar, Effects of variable viscosity and viscous dissipation on laminar convection of a power-law fluid in the entrance region of a semi-circular pipe, Int. J. Heat Mass Transfer 38 (1995) 2225–2232.
[8] T. Min, J.Y. Yoo, H. Choi, Laminar convective heat transfer of a Bingham plastic in a circular pipe. 1. Analytical approach—thermally fully developed flow and thermally developing flow (the Graetz problem extended), Int. J. Heat Mass Transfer 40 (1997) 3025–3037.
[9] T.G. Min, H.G. Choi, J.Y. Yoo, H.C. Choi, Laminar convective heat transfer of a Bingham plastic in a circular pipe. 2. Numerical approach—hydrodynamically developing flow and simultaneously developingflow, Int. J. Heat Mass Transfer 40 (1997) 3689–3701.

[10] T.C. Papanastasiou, Flow of materials with yield, J. Rheol. 31 (1987) 385–404.
[11] A.I. Isayev, C.M. Wong, X. Zeng, Flow of thermoplastics in an annular die under orthogonal oscillations, J. Non-Newt. Fluid Mech. 34 (1990) 375–375.
[12] C.M. Wong, C.H. Chen, A.I. Isayev, Flow of thermoplastics in an annular die under parallel oscillations, Polym. Eng. Sci. 30 (1990) 1574–1584.
[13] J. Dunwoody, The effects of inertia and finite amplitude on oscillatory plane shear flow of K-BKZ fluids such as LDPE melts, J. Non-Newt. Fluid Mech. 65 (1996) 195–220.
[14] F. Ding, A.J. Giacomin, R.B. Bird, C.B. Kweon, Viscous dissipation with fluid inertia in oscillatory shear flow, J. Non-Newt. Fluid Mech. 86 (1999) 359–374.
[15] R.I. Tanner, Engineering Rheology, Clarendon Press, Oxford, 1988.
[16] R.B. Bird, R.C. Amstrong, O. Hassager, Dynamics of polymeric liquids, in: Fluid Mechanics, vol. 1, Wiley, New York, 1977.
[17] J.R. Herrera-Velarde, B. Mena, Oscillatory flows of viscoelastic fluids, Rev. Mex. Fis. 46 (2000) 566–571.
[18] J.R. Herrera-Velarde, R. Zenit, B. Mena, Viscous dissipation of a power law fluid in an oscillatory pipe flow, Rev. Mex. Fis. 47 (2001) 351–356.
[19] J.R. Herrera-Velarde, Transferencia de calor en flujos viscoelasticos escilatorios, Ph.D. thesis, División de Estudios de Posgrado de la Facultad de Ingeniería, Universidad Nacional Autónoma de México, México, 2001.
[20] G. Gruenwald, Plastics: How Structure Determines Properties, Hanser Publishers, New York, 1992.